

Evaluation of Electron Population Terms for $\langle r_{\text{Se}}^{-3} \rangle_{4p}$, $\langle r_{\text{S}}^{-3} \rangle_{3p}$, and $\langle r_{\text{O}}^{-3} \rangle_{2p}$: How Do HOMO and LUMO Shrink or Expand Depending on Nuclear Charges?

Waro Nakanishi,^[a] Satoko Hayashi,^[a] Kenji Narahara,^[a] Daisuke Yamaki,^[b] and Masahiko Hada^[b]

Abstract: Electron population terms $\langle r_N^{-3} \rangle$ are evaluated for $N=\text{Se}$, S , and O . Calculations are performed on HOMO and LUMO constructed by pure atomic 4p(Se), 3p(S), and 2p(O) orbitals, employing the 6-311+G(3d) and/or 6-311++G(3df,3pd) basis sets at the HF, MP2, and DFT (B3LYP) levels. Se^{4+} , Se^{2+} , Se^0 , and Se^{2-} with the O_h symmetry are called G(**A**: Se) and HSe⁺, H_2Se , and HSe⁻ with the $C_{\infty h}$ or C_{2v} symmetry are named G(**B**: Se), here [G(**A+B**: Se) in all]. HOMO and LUMO in G(**A+B**: N) ($N=\text{Se}$, S ,

and O) satisfy the conditions of the calculations for $\langle r_N^{-3} \rangle$. The $\langle r_{\text{Se}}^{-3} \rangle_{4p}$, $\langle r_{\text{S}}^{-3} \rangle_{3p}$, and $\langle r_{\text{O}}^{-3} \rangle_{2p}$ values correlate well with the corresponding MO energies (ϵ_N) for all calculation levels employed. Plots of $\langle r_N^{-3} \rangle_{\text{HOMO}}$ and $\langle r_N^{-3} \rangle_{\text{LUMO}}$ versus $Q(N)$ ($N=\text{Se}$, S , and O) at the HF and MP2 levels are analyzed as two corre-

Keywords: ab initio calculations • absolute shielding tensors • electron population terms • NMR spectroscopy

lations. However, the plots at the DFT level can be analyzed as single correlation. A regression curve is assumed for the analysis. Behaviors of $\langle r_N^{-3} \rangle$ clarify how valence orbitals shrink or expand depending on $Q(N)$. The applicability of $\langle r_N^{-3} \rangle$ is examined to establish a new method that enables us to analyze chemical shifts with the charge effect separately from others. A utility program derived from the Gaussian 03 (NMRANAL-NH03G) is applied to evaluate $\langle r_N^{-3} \rangle$ and examine the applicability to the NMR analysis.

Introduction

Valence orbitals shrink or expand depending on the magnitude of the electron repulsion if those at the same kind of nuclei are compared.^[1] The total magnitude of the electron repulsion at a nucleus (N) in a molecule (M) should be correlated with the electron density at N , which could be evaluated by the nuclear charge ($Q(N)$) in M . The electron population terms $\langle r_N^{-3} \rangle$ will evaluate how molecular orbitals (MOs) shrink or expand. It should be crucial to determine whether $\langle r_N^{-3} \rangle$ or the relative values ($\langle r_N^{-3} \rangle_{\text{rel}}$) correlate with $Q(N)$.

NMR spectroscopy has been established as an extremely powerful tool available to the scientific community;^[2] it's essential for modern chemistry and biology to investigate molecular-level structures and dynamics.^[2] Calculated absolute shielding tensors (σ) become reliable, where total absolute shielding tensors (σ^t) are decomposed into diamagnetic (σ^d) and paramagnetic (σ^p) contributions ($\sigma^t = \sigma^d + \sigma^p$).^[3–5] Employing calculated $\sigma^p(N)$, physical meanings of NMR chemical shifts can be understood more clearly, since $\sigma^p(N)$ is highly sensitive to the structural change around N in M ($\sigma^p(N: M)$). Based on the approximated image derived from Equation (1),^[6,7] $\langle r_N^{-3} \rangle$ in the nuclear-spin electron-orbit interaction terms [$\langle \psi_a | \hat{L}_{z,N} r_N^{-3} | \psi_i \rangle$ and $\langle \psi_i | \hat{L}_{z,N} r_N^{-3} | \psi_a \rangle$] must play an important role to determine the chemical shifts, together with the reciprocal orbital energy gaps [$(\epsilon_a - \epsilon_i)^{-1}$] and the Zeeman terms [$\langle \psi_i | \hat{L}_z | \psi_a \rangle$ and $\langle \psi_a | \hat{L}_z | \psi_i \rangle$].^[2,7] Equation (1) can be rewritten to Equation (2), if $\langle r_N^{-3} \rangle$ can be treated as a constant for N in M .

[a] Prof. Dr. W. Nakanishi, Dr. S. Hayashi, K. Narahara
Department of Material Science and Chemistry
Faculty of Systems Engineering, Wakayama University
930 Sakaedani, Wakayama 640-8510 (Japan)
Fax: (+81)73-457-8253
E-mail: nakanisi@sys.wakayama-u.ac.jp

[b] Dr. D. Yamaki, Prof. Dr. M. Hada
Department of Chemistry, Graduate School of Science
and Engineering, Tokyo Metropolitan University
1-1 Minami-Osawa, Hachioji-shi, Tokyo 192-0397 (Japan)

 Supporting information for this article is available on the WWW under <http://www.chemeurj.org/> or from the author.

$$\begin{aligned} \sigma_{zz}^p(N) = & -(\mu_0 e^2 / 2m_e^2) \sum_i^{\text{occ}} \sum_a^{\text{unocc}} (\epsilon_a - \epsilon_i)^{-1} \\ & \times \{ \langle \psi_i | \hat{L}_z | \psi_a \rangle \langle \psi_a | \hat{L}_{z,N} r_N^{-3} | \psi_i \rangle + \langle \psi_i | \hat{L}_{z,N} r_N^{-3} | \psi_a \rangle \langle \psi_a | \hat{L}_z | \psi_i \rangle \} \end{aligned} \quad (1)$$

$$\sigma_{zz}^p(N) = -(\mu_0 e^2 / 2m_e^2) \langle r_N^{-3} \rangle \sum_i^{\text{occ}} \sum_a^{\text{unocc}} (\varepsilon_a - \varepsilon_i)^{-1} \times \{ \langle \psi_i | \hat{L}_z | \psi_a \rangle \langle \psi_a | \hat{L}_{z,N} | \psi_i \rangle + \langle \psi_i | \hat{L}_{z,N} | \psi_a \rangle \langle \psi_a | \hat{L}_z | \psi_i \rangle \} \quad (2)$$

⁷⁷Se NMR is one of typical methods utilized to determine the structures of selenium containing compounds.^[2,8–11] Indeed, empirical rules are used to assign the spectra on a daily basis, but they are of no use when the physical meanings of the shift values are considered. Plain rules originating from theory are necessary to determine geometric and electronic structures based on the chemical shifts.^[12] If chemical shifts can be discussed separately from the three factors, much more information could be derived from the chemical shifts useful to investigate physical, chemical, and biological sciences.

Atomic 4p(Se) orbitals in the valence MOs mainly control the ⁷⁷Se chemical shifts. To clarify the behavior of $\langle r_N^{-3} \rangle_{4p}$, the values are calculated for HOMO and LUMO constructed by the pure atomic 4p(Se) orbitals in Se⁴⁺, Se²⁺, Se⁰, and Se²⁻ and those in HSe⁺, H₂Se, and HSe⁻. We call the former group **A** [G(A: Se)] herein, since they have no H atoms with the O_h symmetry, and the latter group **B** [G(B: Se)] with the $C_{\infty h}$ or C_{2v} symmetry due to the H atom(s)^[13] [G(A+B: Se) in all]. Similar calculations are performed on sulfur and oxygen species: $\langle r_S^{-3} \rangle_{3p}$ and $\langle r_O^{-3} \rangle_{2p}$ are calculated for G(A+B: S) and G(A+B: O), respectively, for convenience of comparison. The values are connected to $Q(N)$ in the expectation that $\langle r_N^{-3} \rangle$ can be approximately estimated based on $Q(N)$.

Here, we report the results of the calculations on $\langle r_N^{-3} \rangle$ for HOMO and LUMO constructed by pure atomic 4p(Se) orbitals in G(A+B: Se), 3p(S) in G(A+B: S), and 2p(O) in G(A+B: O). Correlations of $\langle r_N^{-3} \rangle$ with $Q(N)$ (N =Se, S, and O) and the corresponding MO energies (ε_N) in G(A+B: N) are discussed. It can be assumed that the valence orbitals shrink or expand depending on $Q(N)$ through evaluation of $\langle r_N^{-3} \rangle$. The results will open the door to develop a new method to analyze the NMR chemical shifts.

Results and Discussion

Calculation method: The 6-311+G(3d) and 6-311++G(3df,3pd) basis sets in the Gaussian 03 program^[14,15] are employed for G(A+B: N) (N of Se, S, and O). Calculations are performed at the Hartree–Fock (HF) level,^[16] the Møller–Plesset second order energy correlation (MP2) level,^[17] and/or the density functional theory (DFT) level of the Becke three-parameter hybrid functionals with the Lee–Yang–Parr correlation functional (B3LYP).^[18] The $\langle r_N^{-3} \rangle_{ij}$ values averaged by ψ_i and ψ_j are calculated according to Equation (3), although $\langle r_N^{-3} \rangle_{\text{HOMO}}$ ($\psi_i=\psi_j=\text{HOMO}$) and $\langle r_N^{-3} \rangle_{\text{LUMO}}$ ($\psi_i=\psi_j=\text{LUMO}$) are used in place of $\langle r_N^{-3} \rangle_{ij}$, if they are suitable.^[19] The utility program derived from the Gaussian 03 program are applied to calculate the $\langle r_N^{-3} \rangle$ values (NMRA-NH03G).^[20,21]

$$\langle r_N^{-3} \rangle_{ij} = \langle \psi_i | r_N^{-3} | \psi_j \rangle \quad (3)$$

Evaluation of electron population terms $\langle r_N^{-3} \rangle$ ($N=\text{Se, S, and O}$): Figure 1 illustrates $\psi_{16}-\psi_{18}$ for Se⁰ at the singlet state, which are constructed by the pure atomic 4p(Se) orbitals. ψ_{16} and ψ_{17} are occupied and ψ_{18} is vacant. MOs and the energies for Se⁴⁺, Se²⁺, and Se²⁻ are closely related to those for Se⁰. While $\psi_{16}-\psi_{18}$ are vacant in Se⁴⁺, ψ_{16} is occupied and ψ_{17} and ψ_{18} are vacant in Se²⁺, and $\psi_{16}-\psi_{18}$ are occupied in Se²⁻.

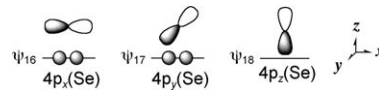


Figure 1. HOMO (ψ_{16} and ψ_{17}) and LUMO (ψ_{18}) illustrated for Se⁰ at the singlet state.

The $\langle r_N^{-3} \rangle$ values are calculated for HOMO and LUMO constructed by pure atomic 4p(Se) orbitals in G(A+B: Se), by pure 3p(S) in G(A+B: S), and by pure 2p(O) in G(A+B: O) at the singlet state according to Equation (3). Table 1 summarizes the results calculated with the 6-311+G(3d) basis sets for G(A+B: Se) at the HF, MP2, and B3LYP levels and for G(A+B: S and O) at the B3LYP level. The $\langle r_N^{-3} \rangle_{\text{rel}}$ values are also obtained assuming $\langle r_N^{-3} \rangle_{\text{HOMO}}=1.000$ for each N^0 of G(A: N). Table 1 summarizes the $\langle r_N^{-3} \rangle_{\text{rel}}$ values ($\langle r_N^{-3} \rangle_{\text{HOMO,rel}}$ and $\langle r_N^{-3} \rangle_{\text{LUMO,rel}}$), together with the corresponding MO energies (ε_N : $\varepsilon_{N:\text{HOMO}}$ and $\varepsilon_{N:\text{LUMO}}$) and $Q(N)$ calculated employing the natural population analysis^[14] with the same methods. Data for G(A+B: S and O) at the HF and MP2 levels are given in the Supporting Information (Tables S1 and S2). The B3LYP/6-311++G(3df,3pd) method is also applied to G(A+B: Se and S) for ease of comparison. The results are shown in the Supporting Information (Table S3). The $\langle r_N^{-3} \rangle$ values for HOMO and LUMO of Se²⁺ and Se⁰ at the triplet state are similarly calculated with the B3LYP/6-311+G(3d) method. The $\langle r_N^{-3} \rangle_{\text{rel}}$ values at the triplet state are also obtained assuming $\langle r_N^{-3} \rangle_{\text{HOMO}}=1.000$ for Se⁰ at the singlet state (see Table S4 in the Supporting Information for results, containing the average values).

Before discussion of the correlation between $\langle r_N^{-3} \rangle$ and $Q(N)$, it is important to discuss the correlation between $\langle r_N^{-3} \rangle$ and ε_N .

Correlations between $\langle r_N^{-3} \rangle$ and ε_N ($N=\text{Se, S, and O}$): Figure 2 shows the plots of $\langle r_N^{-3} \rangle_{\text{HOMO}}$ and $\langle r_N^{-3} \rangle_{\text{LUMO}}$ versus corresponding ε_N for $N=\text{Se, S, and O}$, calculated with the HF/6-311+G(3d) method. The correlations are very good. Table 2 shows the results (entries 1–3). The correlations for the data calculated with the MP2/6-311+G(3d) method are very close to those obtained by the HF/6-311+G(3d) method. The results calculated with the MP2/6-311+G(3d) methods are also shown in Table 2 (entries 4–6). The plots with the MP2/6-311+G(3d) method is given in the Supporting Information (Figure S1). Figure 3 shows the plots of $\langle r_N^{-3} \rangle_{\text{HOMO}}$ and $\langle r_N^{-3} \rangle_{\text{LUMO}}$ versus ε_N for $N=\text{Se, S, and O}$, calculated with the B3LYP/6-311+G(3d) method. The correla-

Table 1. $\langle r_N^{-3} \rangle_{\text{HOMO}}$, $\langle r_N^{-3} \rangle_{\text{HOMO:rel}}$, $\langle r_N^{-3} \rangle_{\text{LUMO}}$, and $\langle r_N^{-3} \rangle_{\text{LUMO:rel}}$ values for Se^{4+} , Se^{2+} , Se^0 , and Se^{2-} ($\mathbf{G(A: Se)}$), HSe^+ , H_2Se , and HSe^- ($\mathbf{G(B: Se)}$), $\mathbf{G(A+B: S)}$, and $\mathbf{G(A+B: O)}$ at the singlet state, together with $\varepsilon_{N:\text{HOMO}}$, $\varepsilon_{N:\text{LUMO}}$, and $Q(N)$ ($N = \text{Se}, \text{S}$, and O).

Species	$\langle r_N^{-3} \rangle_{\text{HOMO}}$ [a_0^{-3}]	$\langle r_N^{-3} \rangle_{\text{rel}}^{[a,b]}$ [a_0^{-3}]	$\langle r_N^{-3} \rangle_{\text{LUMO}}$ [a_0^{-3}]	$\langle r_N^{-3} \rangle_{\text{rel}}^{[b,c]}$	$\varepsilon_{N:\text{HOMO}}$ [au]	$\varepsilon_{N:\text{LUMO}}$ [au]	$Q(N)^{[d]}$
HF/6-311+G(3d)							
Se^{4+}			14.082	1.542		-1.526	4
Se^{2+}	12.307	1.347	10.540	1.154	-1.067	-0.730	2
Se^0	9.133	1.000 ^[e]	6.798	0.744	-0.373	-0.079	0
Se^{2-}	6.340	0.694			0.114		-2
HSe^+	10.382	1.137	8.443	0.924	-0.684	-0.370	0.933
H_2Se	8.717	0.954			-0.358		-0.131
HSe^-	7.490	0.820			-0.090		-1.000
MP2/6-311+G(3d)							
Se^{4+}			14.082	1.542		-1.526	4
Se^{2+}	12.307	1.347	10.540	1.154	-1.067	-0.730	2
Se^0	9.133	1.000 ^[e]	6.798	0.744	-0.373	-0.079	0
Se^{2-}	6.340	0.694			0.114		-2
HSe^+	10.380	1.137	8.441	0.924	-0.684	-0.370	0.925
H_2Se	8.441	0.955			-0.358		-0.135
HSe^-	7.498	0.821			-0.090		-1.000
B3LYP/6-311+G(3d)							
Se^{4+}			17.764	1.737		-1.731	4
Se^{2+}	13.798	1.349	13.869	1.356	-0.944	-0.914	2
Se^0	10.228	1.000 ^[e]	10.242	1.001	-0.264	-0.237	0
Se^{2-}	7.147	0.699			0.181		-2
HSe^+	11.630	1.137	11.659	1.140	-0.568	-0.540	0.907
H_2Se	9.760	0.954			-0.251		-0.190
HSe^-	8.373	0.819			0.002		-1.030
S^{4+}			9.141	1.773		-1.921	4
S^{2+}	7.248	1.365	7.160	1.349	-1.041	-0.997	2
S^0	5.308	1.000 ^[e]	5.200	0.980	-0.283	-0.248	0
S^{2-}	3.690	0.695			0.204		-2
HS^+	6.014	1.133	5.910	1.113	-0.615	-0.576	0.858
H_2S	4.990	0.940			-0.266		-0.275
HS^-	4.306	0.811			0.007		-1.073
O^{4+}			9.491	1.912		-3.201	4
O^{2+}	7.070	1.424	6.717	1.353	-1.628	-1.525	2
O^0	4.963	1.000 ^[e]	4.608	0.928	-0.381	-0.301	0
O^{2-}	3.402	0.686			0.341		-2
OH^+	5.479	1.104	5.133	1.034	-0.851	-0.764	0.482
H_2O	4.364	0.879			-0.321		-0.922
OH^-	3.875	0.781			0.048		-1.369

[a] $\langle r_N^{-3} \rangle_{\text{HOMO:rel}}$. [b] $\langle r_N^{-3} \rangle_{\text{HOMO}} = 1.000$ for each N^0 of $\mathbf{G(A: N)}$. [c] $\langle r_N^{-3} \rangle_{\text{LUMO:rel}}$. [d] Nuclear charge calculated with the natural population analysis for $\mathbf{G(B: N)}$. [e] Chosen as the standard.

tions are excellent (see Table 2, entries 7–9). These results demonstrate that $\langle r_N^{-3} \rangle_{\text{HOMO}}$ and $\langle r_N^{-3} \rangle_{\text{LUMO}}$ ($N = \text{Se}, \text{S}$, and O) are well correlated with ε_N , irrespective of the calculation methods.

After elucidating the relationship between $\langle r_N^{-3} \rangle$ and ε_N , the correlation between $\langle r_N^{-3} \rangle$ and $Q(N)$ needs to be clarified, where ε_N cannot be assigned to an atom N in \mathbf{M} , whereas $Q(N)$ can be.

Correlations between $\langle r_N^{-3} \rangle$ and $Q(N)$ ($N = \text{Se}, \text{S}$, and O): Figure 4 shows the plots of $\langle r_{\text{Se}}^{-3} \rangle_{\text{HOMO:rel}}$ and $\langle r_{\text{Se}}^{-3} \rangle_{\text{LUMO:rel}}$ versus $Q(\text{Se})$ for $\mathbf{G(A+B: Se)}$, calculated with the HF/6-311+G(3d) method. Figure 5 shows the plots for those calculated with the B3LYP/6-311+G(3d) method.

$$y = A_{\text{rel}} \exp(\alpha_{\text{rel}}x) + (1 - A_{\text{rel}}) \quad (4)$$

$$y = A_{\text{rel}} \exp(\alpha_{\text{rel}}x) + B_{\text{rel}} \quad (5)$$

The plot for $\langle r_{\text{Se}}^{-3} \rangle_{\text{HOMO:rel}}$ of $\mathbf{G(A+B: Se)}$ calculated with the HF/6-311+G(3d) method in Figure 4 is analyzed incorporating the regression curve shown in Equation (4),^[22] where x and y stand for $Q(\text{Se})$ and $\langle r_{\text{Se}}^{-3} \rangle_{\text{rel}}$, respectively. The Equation includes $(x,y) = (Q(N), \langle r_N^{-3} \rangle_{\text{rel}}) = (0,1)$. The correlation is very good. Table 3 shows the $(A_{\text{rel}}, \alpha_{\text{rel}})$ values (entry 1), where H and L stand for HOMO and LUMO, respectively. Figure 4 also contains the plot of $\langle r_{\text{Se}}^{-3} \rangle_{\text{LUMO:rel}}$ versus $Q(\text{Se})$ for $\mathbf{G(A+B: Se)}$, which should be further analyzed as another correlation; this can be achieved by applying Equation (5), which does not satisfy $(x,y) = (0,1)$. The correlation is also very good. Table 3 shows the $(A_{\text{rel}}, \alpha_{\text{rel}})$ values with B_{rel} in the footnote (entry 2). The plots of $\langle r_{\text{Se}}^{-3} \rangle_{\text{HOMO:rel}}$ and $\langle r_{\text{Se}}^{-3} \rangle_{\text{LUMO:rel}}$ versus $Q(\text{Se})$ for $\mathbf{G(A: Se)}$ are similarly analyzed. The results are given in Table 3 (entries 3 and 4). The results for $\mathbf{G(A+B: Se)}$ are essentially the same as those for $\mathbf{G(A: Se)}$. The plots of $\langle r_{\text{Se}}^{-3} \rangle_{\text{HOMO:rel}}$ and $\langle r_{\text{Se}}^{-3} \rangle_{\text{LUMO:rel}}$ versus $Q(\text{Se})$, calculated with the MP2/6-311+G(3d) method, are shown in the Supporting Information (Figure S2). Table 3 summarizes the correlations (entries 5–8). The results with the MP2/6-311+G(3d) method are essentially the same as those with the HF/6-311+G(3d) method.

The plots of $\langle r_{\text{Se}}^{-3} \rangle_{\text{HOMO:rel}}$ and $\langle r_{\text{Se}}^{-3} \rangle_{\text{LUMO:rel}}$ versus $Q(\text{Se})$ for $\mathbf{G(A+B: Se)}$ calculated with the B3LYP/6-311+G(3d) method shown in Figure 5 can fortunately be analyzed as a single correlation. Equation (4) is applied for the analysis. The correlation is excellent ($R^2 = 0.999$). Table 3 shows the results (entry 9).^[23] The Table also contains the correlations for the plots of $\langle r_{\text{Se}}^{-3} \rangle_{\text{HOMO:rel}}$ and $\langle r_{\text{Se}}^{-3} \rangle_{\text{LUMO:rel}}$ in $\mathbf{G(A: Se)}$ (entry 10). The results for $\mathbf{G(A+B: Se)}$ are very similar to those for $\mathbf{G(A: Se)}$. The correlation for the plot of $\langle r_{\text{Se}}^{-3} \rangle_{\text{HOMO:rel}}$ in $\mathbf{G(A: Se)}$ is also given in Table 3 (entry 11). The results show that there are no substantial differences

Table 2. Correlations in $\langle r_N^{-3} \rangle$ and ε_N for $N=\text{O}, \text{S}$, and Se .^[a]

No	y	x	a	b	R^2	Comment
HF/6-311+G(3d)						
1	$\langle r_{\text{Se}}^{-3} \rangle$	ε_{Se}	-4.881	6.903	0.988	G(A+B: Se)
2	$\langle r_{\text{S}}^{-3} \rangle$	ε_{S}	-2.413	3.523	0.988	G(A+B: S)
3	$\langle r_{\text{O}}^{-3} \rangle$	ε_{O}	-1.776	3.354	0.971	G(A+B: O)
MP2/6-311+G(3d)						
4	$\langle r_{\text{Se}}^{-3} \rangle$	ε_{Se}	-4.879	6.905	0.988	G(A+B: Se)
5	$\langle r_{\text{S}}^{-3} \rangle$	ε_{S}	-2.413	3.524	0.988	G(A+B: S)
6	$\langle r_{\text{O}}^{-3} \rangle$	ε_{O}	-1.774	3.357	0.970	G(A+B: O)
B3LYP/6-311+G(3d)						
7	$\langle r_{\text{Se}}^{-3} \rangle$	ε_{Se}	-5.506	8.547	0.993	G(A+B: Se)
8	$\langle r_{\text{S}}^{-3} \rangle$	ε_{S}	-2.680	4.387	0.995	G(A+B: S)
9	$\langle r_{\text{O}}^{-3} \rangle$	ε_{O}	-1.742	4.016	0.992	G(A+B: O)
10	$\langle r_{\text{Se}}^{-3} \rangle$	$\langle r_{\text{Se}}^{-3} \rangle$	0.540	-0.256	0.998	G(A+B)
11	$\langle r_{\text{O}}^{-3} \rangle$	$\langle r_{\text{Se}}^{-3} \rangle$	0.581	-1.138	0.976	G(A+B)
12	$\langle r_{\text{S}}^{-3} \rangle$	$\langle r_{\text{O}}^{-3} \rangle$	1.081	-0.894	0.987	G(A+B)
13	ε_{S}	ε_{Se}	1.112	0.012	1.000	G(A+B)
14	ε_{O}	ε_{Se}	1.853	0.118	0.994	G(A+B)

[a] Analyzed according to $y=ax+b$ (R^2 : square of correlation coefficient).

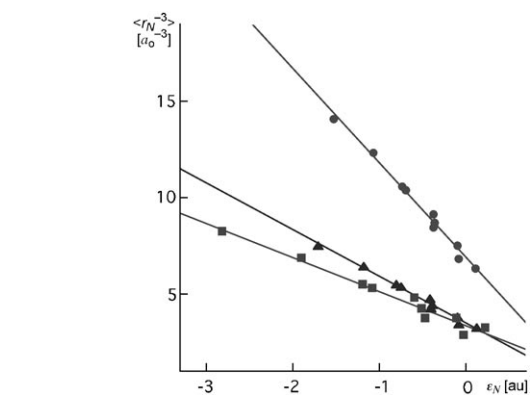


Figure 2. Plots of $\langle r_N^{-3} \rangle$ versus ε_N for HOMO and LUMO in G(A+B: N) calculated with the HF/6-311+G(3d) method: ● for $N=\text{Se}$, ▲ for $N=\text{S}$, and ■ for $N=\text{O}$.

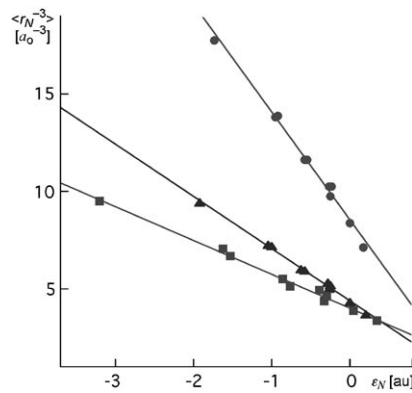


Figure 3. Plots of $\langle r_N^{-3} \rangle$ versus ε_N for HOMO and LUMO in G(A+B: N) calculated with the B3LYP/6-311+G(3d) method: ● for $N=\text{Se}$, ▲ for $N=\text{S}$, and ■ for $N=\text{O}$.

between the three plots. Similar plots of G(A+B: N) versus $Q(N)$ ($N=\text{S}$ and O) are analyzed as single correlation for each as shown in the Supporting Information (Figures S4

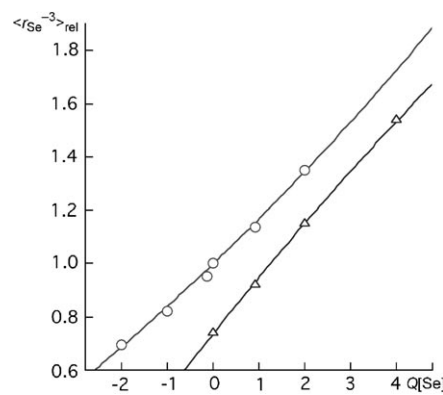


Figure 4. Plots of $\langle r_{\text{Se}}^{-3} \rangle_{\text{HOMO,rel}}$ and $\langle r_{\text{Se}}^{-3} \rangle_{\text{LUMO,rel}}$ versus $Q(\text{Se})$ for G(A+B: Se) calculated with the HF/6-311+G(3d) method: ○ for HOMO and △ for LUMO.

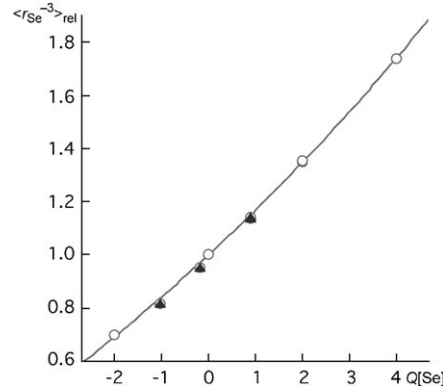


Figure 5. Plots of $\langle r_{\text{Se}}^{-3} \rangle_{\text{HOMO,rel}}$ and $\langle r_{\text{Se}}^{-3} \rangle_{\text{LUMO,rel}}$ versus $Q(\text{Se})$ calculated with the B3LYP/6-311+G(3d) method: ○ for G(A+B: Se) and ▲ for G(B: Se). Data for $\langle r_{\text{Se}}^{-3} \rangle_{\text{LUMO,rel}}$ and $\langle r_{\text{Se}}^{-3} \rangle_{\text{HOMO,rel}}$ are substantially equal for Se^0 , Se^{2+} , and HSe^+ .

and $\text{S}5$). The correlations are given in Table 3 (entries 12–17). The Table also collects the $A_{\text{rel}}\alpha_{\text{rel}}$ values for the correlations, which correspond to the charge dependence of $\langle r_N^{-3} \rangle_{\text{rel}}$ at $Q(N)=0$.^[24]

Equation (6) should be applied when $\langle r_N^{-3} \rangle_{\text{HOMO}}$ and $\langle r_N^{-3} \rangle_{\text{LUMO}}$ are plotted versus $Q(N)$. In these cases, Equation (6) will be obtained by multiplying the both sides of Equations (4) or (5) by $\langle r_N^{-3} \rangle_{\text{HOMO}}(N^0)$ ($=k_o(N^0)$) ($N=\text{Se}, \text{S}$, or O), used as the standard values. Therefore, Equations (7) and (8) are derived

from Equations (4) and (5), respectively:

$$y = A \exp(ax) + B \quad (6)$$

Table 3. A_{rel} , α_{rel} , and $A_{\text{rel}}\alpha_{\text{rel}}$ values for G(A and/or B: N) ($N=\text{Se}, \text{S}$, and O).^[a,b]

No.	H and/or L ^[c]	A_{rel}	α_{rel}	R^2 ^[d]	$A_{\text{rel}}\alpha_{\text{rel}}$ ^[e]	Comment
HF/6-311+G(3d)						
1	HOMO	3.344	0.0489	0.995	0.1635	G(A+B: Se)
2	LUMO	-5.104	-0.0423	0.999	0.2159	G(A+B: Se) ^[f]
3	HOMO	2.555	0.0637	1.000	0.1628	G(A: Se)
4	LUMO	-7.636	-0.0276	1.000	0.2108	G(A: Se) ^[g]
MP2/6-311+G(3d)						
5	HOMO	3.294	0.0497	0.995	0.1637	G(A+B: Se)
6	LUMO	-5.081	-0.0425	0.999	0.2159	G(A+B: Se) ^[h]
7	HOMO	2.555	0.0637	1.000	0.1628	G(A: Se)
8	LUMO	-7.636	-0.0276	1.000	0.2108	G(A: Se) ^[i]
B3LYP/6-311+G(3d)						
9	H + L ^[c]	2.713	0.0602	0.999	0.1633	G(A+B: Se)
10	H + L ^[c]	2.580	0.0631	1.000	0.1628	G(A: Se)
11	HOMO	2.196	0.0738	1.000	0.1621	G(A: Se)
12	H + L ^[c]	2.130	0.0772	0.997	0.1644	G(A+B: S)
13	H + L ^[c]	2.111	0.0781	0.999	0.1649	G(A: S)
14	HOMO	1.843	0.0904	1.000	0.1666	G(A: S)
15	H + L ^[c]	1.245	0.1370	0.990	0.1706	G(A+B: O)
16	H + L ^[c]	1.368	0.1273	0.992	0.1741	G(A: O)
17	HOMO	1.213	0.1500	1.000	0.1820	G(A: O)
B3LYP/6-311++G(3df,3pd)						
18	H + L ^[c]	2.641	0.0615	0.998	0.1624	G(A+B: Se)
19	H + L ^[c]	2.545	0.0637	1.000	0.1621	G(A: Se)
20	HOMO	2.282	0.0709	1.000	0.1618	G(A: Se)
21	H + L ^[c]	2.367	0.0682	0.996	0.1614	G(A+B: S)
22	H + L ^[c]	2.289	0.0705	0.999	0.1614	G(A: S)
23	HOMO	1.909	0.0856	1.000	0.1634	G(A: S)

[a] According to Equations (4) and/or (5). [b] B_{rel} in the footnote. [c] H stands for HOMO and L for LUMO.

[d] Square of correlation coefficient in $y=ax+b$ (R^2). [e] $(dy/dx)_{x=0}$. [f] $B_{\text{rel}}=5.840$. [g] $B_{\text{rel}}=8.380$. [h] $B_{\text{rel}}=5.818$. [i] $B_{\text{rel}}=8.380$.

$$A = k_0(N^0) \cdot A_{\text{rel}}, \alpha = \alpha_{\text{rel}}, \text{ and } B = k_0(N^0) \cdot (1 - A_{\text{rel}}) \quad (7)$$

$$A = k_0(N^0) \cdot A_{\text{rel}}, \alpha = \alpha_{\text{rel}}, \text{ and } B = k_0(N^0) \cdot B_{\text{rel}} \quad (8)$$

$$(k_0(N^0) = \langle r_N^{-3} \rangle_{\text{HOMO}}(N^0) \quad (N=\text{Se}, \text{S}, \text{or O}))$$

It would be interesting if the magnitudes of $\langle r_N^{-3} \rangle$ are not so close to those of $\langle r_{\text{Se}}^{-3} \rangle$ but close to those of $\langle r_{\text{O}}^{-3} \rangle$ for G(A+B) when calculated with the B3LYP/6-311+G(3d) method (entries 10–12 in Table 2; Figure S6, Supporting Information). The value from the covalent radii of N ($r_{\text{cov},N}$) may not be valid in $\langle r_N^{-3} \rangle$ for $N=\text{Se}, \text{S}$ and O. On the other hand, $\varepsilon_s(G(\mathbf{A}+\mathbf{B}))$ correlate well with $\varepsilon_{\text{Se}}(G(\mathbf{A}+\mathbf{B}))$, compared with the case of $\varepsilon_{\text{O}}(G(\mathbf{A}+\mathbf{B}))$ (entries 13 and 14 in Table 3, Figure S7 in the Supporting Information). The data calculated with the B3LYP/6-311++G(3df,3pd) method are similarly plotted for G(A+B: Se) and G(A+B: S). The results are very close to those of the B3LYP/6-311+G(3d) method. Table 3 also collects the correlations (entries 18–23).

After establishment of the correlation between $\langle r_N^{-3} \rangle$ and $Q(N)$, the applicability of $\langle r_N^{-3} \rangle$ is subsequently considered to develop a new method to analyze NMR chemical shifts separately by the $Q(N)$ factor from others.

Applicability of $\langle r_N^{-3} \rangle$ to NMR analysis: The applicability of $\langle r_N^{-3} \rangle$ for NMR analysis is exemplified by SeH_2 .^[25] Since σ^p are evaluated by the coupled Hartree-Fock (CPHF) method

in the Gaussian 03 program, they can be decomposed into the contribution of the occupied orbitals or the orbital-orbital transitions^[7] as shown in Equation (9).

$$\sigma^p = \sum_i^{\text{occ}} \sum_a^{\text{unocc}} \sigma_{i \rightarrow a}^p \quad (9)$$

$$= \sum_i^{\text{occ}} \sigma_i^p$$

Figure 6 shows the ψ_{18} (HOMO) to ψ_{20} (LUMO+1) transition in SeH_2 .^[26] The molecular plane of SeH_2 is set to the xy plane with the bisected direction of HSeH to the x axis, here. Consequently, ψ_{18} (HOMO) is the pure $4p_z(\text{Se})$ and ψ_{20} (LUMO+1) is constructed by $4p_y(\text{Se})$ and h_2 (H_2), as shown in Figure 7. Therefore, the $\psi_{18} \rightarrow \psi_{20}$ transition corresponds to $\sigma^p(\text{Se})_{xx}$, which contributes the largest downfield shift to $\sigma^p(\text{Se})$. The transition amounts to -1345 ppm when calculated

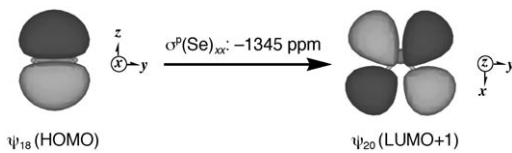


Figure 6. ψ_{18} (HOMO) to ψ_{20} (LUMO+1) transition in SeH_2 , contributing to $\sigma^p(\text{Se})_{xx}$.

with the DFT-GIAO method employing the 6-311+(3d) basis sets.

According to Equation (1), $\langle \psi_{20} | \hat{L}_{z,N} r_N^{-3} | \psi_{18} \rangle$ and $\langle \psi_{18} | \hat{L}_{z,N} r_N^{-3} | \psi_{20} \rangle$ have to be determined for the $\psi_{18} \rightarrow \psi_{20}$ transition, which would be reduced to Equation (3) with $i=18$ and $j=20$ for SeH_2 , although the angular momentum operator ($\hat{L}_{z,N}$) must also be considered. The $\langle r_{\text{Se}}^{-3} \rangle_{\text{HOMO},\text{rel}}$ and $\langle r_{\text{Se}}^{-3} \rangle_{\text{LUMO},\text{rel}}$ values are correlated well with $Q(N)$ and substantially equal with each other, if calculated with the B3LYP/6-311+G(3d) method. It would be possible to analyze the ^{77}Se NMR chemical shifts separately by the factor of $Q(N)$ by applying the GIAO-DFT (B3LYP) method,^[27] if the shift values are predominantly controlled by $4p(\text{Se})$ in occupied and unoccupied MOs.

Conclusion

Straightforward rules are necessary to determine geometric and electronic structures based on the chemical shifts, which

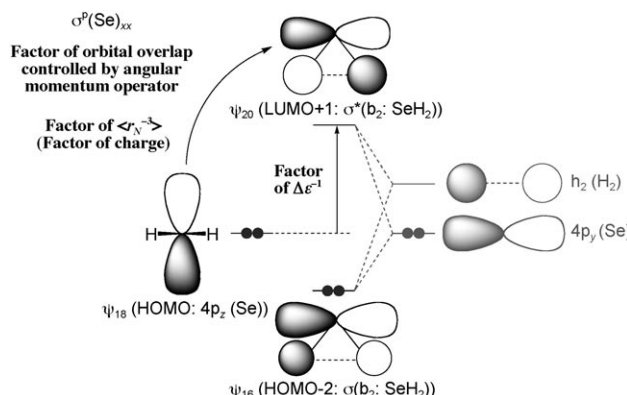


Figure 7. Illustration for the formation of ψ_{16} and ψ_{20} from $4p_y(\text{Se})$ and $h_2(\text{H}_2)$ in SeH_2 , together with factors to control the ^{77}Se chemical shifts exemplified by the $\psi_{18} \rightarrow \psi_{20}$ transition.

are founded on theory. Much more information will be derived from the chemical shifts useful to investigate physical, chemical, and biological sciences, if chemical shifts are analyzed separately by the factors of charges, reciprocal orbital energy gaps, and orbital overlaps. As a first step to establish such rules, behaviors of electron population terms, that is, $\langle r_N^{-3} \rangle$ ($N = \text{Se, S, and O}$), are elucidated for pure p-type atomic orbitals in HOMO and LUMO. The $\langle r_N^{-3} \rangle_{\text{HOMO}}$ and $\langle r_N^{-3} \rangle_{\text{LUMO}}$ values are well correlated with ε_N irrespective of the calculation levels. They also correlated well with $Q(N)$. The plots are analyzed as two correlations for the values calculated at the HF and MP2 levels. However, those for the data at the B3LYP level can be analyzed as single correlation. Namely, both $\langle r_N^{-3} \rangle_{\text{HOMO}}$ and $\langle r_N^{-3} \rangle_{\text{LUMO}}$ can be predicted by $Q(N)$. While ε_N cannot be assigned to the specified N in M , $Q(N)$ can be calculated for the specified N . The results will establish a new method to analyze the chemical shifts separately by the factor of charges, if $\sigma^0(N)$ are calculated with the DFT (B3LYP) method.

Investigations are in progress to establish a new method to analyze the chemical shifts separately by the three factors.

Acknowledgements

This work was partially supported by a Grant-in-Aid for Scientific Research (Nos. 16550038, 19550041, and 20550042) from the Ministry of Education, Culture, Sports, Science, and Technology, Japan.

- [1] a) *Molecular Quantum Mechanics*, 4th ed. (Eds.: P. W. Atkins, R. S. Friedman), Oxford, New York, **2005**; b) *Quantum Mechanics in Chemistry* (Eds.: J. Simons, J. Nichols), Oxford, New York, **1997**.
- [2] a) *Encyclopedia of Nuclear Magnetic Resonance* (Eds.: D. M. Grant, R. K. Harris), Wiley, New York, **1996**; b) *Nuclear Magnetic Shieldings and Molecular Structure* (Ed.: J. A. Tossell), Kluwer Academic Publishers, Dordrecht, **1993**; c) *Calculation of NMR and EPR Parameters; Theory and Applications* (Eds.: M. Kaupp, M. Bühl, V. G. Malkin), Wiley-VCH, Weinheim, **2004**.

[3] Although the contribution of relativistic terms has been pointed out for heavier atoms, the perturbation would be small for the selenium nucleus: R. Fukuda, M. Hada, H. Nakatsuji, *J. Chem. Phys.* **2003**, *118*, 1015–1026; R. Fukuda, M. Hada, H. Nakatsuji, *J. Chem. Phys.* **2003**, *118*, 1027–1035; S. Tanaka, M. Sugimoto, H. Takashima, M. Hada, H. Nakatsuji, *Bull. Chem. Soc. Jpn.* **1996**, *69*, 953–959; C. C. Ballard, M. Hada, H. Kaneko, H. Nakatsuji, *Chem. Phys. Lett.* **1996**, *254*, 170–178; H. Nakatsuji, M. Hada, H. Kaneko, C. C. Ballard, *Chem. Phys. Lett.* **1996**, *255*, 195–202; M. Hada, H. Kaneko, H. Nakatsuji, *Chem. Phys. Lett.* **1996**, *261*, 7–12.

[4] K. Kanda, H. Nakatsuji, T. Yonezawa, *J. Am. Chem. Soc.* **1984**, *106*, 5888–5892.

[5] This decomposition includes small arbitrariness due to the coordinate origin dependence, though it does not damage our chemical analyses and insights into the ^{77}Se NMR spectroscopy.

[6] σ^0 and σ^d are exactly expressed by the Ramsey's Equation, and they are approximately calculated in the framework of the Hartree-Fock (H-F) and DFT theory: N. F. Ramsey, *Phys. Rev.* **1950**, *77*, 567; N. F. Ramsey, *Phys. Rev.* **1950**, *78*, 699–703; N. F. Ramsey, *Phys. Rev.* **1951**, *83*, 540–541; N. F. Ramsey, E. M. Purcell, *Phys. Rev.* **1952**, *85*, 143–144; N. F. Ramsey, *Phys. Rev.* **1953**, *91*, 303–307; N. F. Ramsey, *Phys. Rev.* **1952**, *86*, 243–246.

[7] Based on the second-order perturbation theory at the level of the HF and single-excitation CI approximation, σ^0_{i-a} on a resonance nucleus N is shown to be proportional to reciprocal orbital energy gap $(\varepsilon_a - \varepsilon_i)^{-1}$. $\sigma^0_{zz}(N)$ are approximately given by Equation (1), where ψ_k is the k -th orbital function, $\hat{L}_{z,N}$ is orbital angular momentum around the resonance nucleus, and r_N is the distance from the nucleus N .

[8] a) *Organic Selenium Compounds: Their Chemistry and Biology* (Eds.: D. L. Klayman, W. H. H. Günther), Wiley, New York, **1973**; b) *The Chemistry of Organic Selenium and Tellurium Compounds*, Vol. 1 (Eds.: S. Patai, Z. Rappoport), Wiley, New York, **1986**; *The Chemistry of Organic Selenium and Tellurium Compounds*, Vol. 2 (Ed.: S. Patai), Wiley, New York, **1987**; c) *Organoselenium Chemistry* (Ed.: D. Liotta), Wiley-Interscience, New York, **1987**; d) *Organoselenium Chemistry, A Practical Approach* (Ed.: T. G. Back), Oxford University Press, Oxford, **1999**; e) *Organoselenium Chemistry Modern Developments in Organic Synthesis*, *Top. Curr. Chem.*, Vol. 208 (Ed.: T. Wirth), Springer, Heidelberg, **2000**.

[9] a) W. McFarlane, R. J. Wood, *J. Chem. Soc. Dalton Trans.* **1972**, 1397–1402; b) H. Iwamura, W. Nakanishi, *J. Syn. Org. Chem. Jpn.* **1981**, *39*, 795–804; c) *The Chemistry of Organic Selenium and Tellurium Compounds*, Vol. 1 (Eds.: S. Patai, Z. Rappoport), Wiley, New York, **1986**, Chapter 6; d) *Compilation of Reported ⁷⁷Se NMR Chemical Shifts* (Eds.: T. M. Klapötke, M. Broschag), Wiley, New York, **1996**; e) H. Duddeck, *Prog. Nucl. Magn. Reson. Spectrosc.* **1995**, *27*, 1–323.

[10] a) S. Gronowitz, A. Konar, A.-B. Hörmfeldt, *Org. Magn. Reson.* **1977**, *9*, 213–217; b) G. P. Mullen, N. P. Luthra, R. B. Dunlap, J. D. Odom, *J. Org. Chem.* **1985**, *50*, 811–816; c) G. A. Kalabin, D. F. Kushnarev, V. M. Bzesovsky, G. A. Tschmutova, *Org. Magn. Reson.* **1979**, *12*, 598–604; d) G. A. Kalabin, D. F. Kushnarev, T. G. Mannafav, *Zh. Org. Khim.* **1980**, *16*, 505–512; e) W. Nakanishi, S. Hayashi, T. Uehara, *Eur. J. Org. Chem.* **2001**, 3933–3943.

[11] a) S. Hayashi, W. Nakanishi, *J. Org. Chem.* **1999**, *64*, 6688–6696; b) W. Nakanishi, S. Hayashi, *Chem. Lett.* **1998**, 523–524; c) W. Nakanishi, S. Hayashi, *J. Phys. Chem. A* **1999**, *103*, 6074–6081.

[12] a) W. Nakanishi, S. Hayashi, M. Hada, *Chem. Eur. J.* **2007**, *13*, 5282–5293; b) W. Nakanishi, S. Hayashi, D. Shimizu, M. Hada, *Chem. Eur. J.* **2006**, *12*, 3829–3846; S. Hayashi, W. Nakanishi, *Bioinorganic Chemistry and Applications*, **2006**, doi:10.1155/BCA/2006/79327.

[13] Pure p atomic orbitals of G(B) might be affected slightly by the H atom(s) through the polarization functions in the calculations, which would slightly change $\langle r_N^{-3} \rangle$.

[14] Gaussian 03, Revision D.02, M. J. Frisch, G. W. Trucks, H. B. Schlegel, G. E. Scuseria, M. A. Robb, J. R. Cheeseman, J. A. Montgomery Jr., T. Vreven, K. N. Kudin, J. C. Burant, J. M. Millam, S. S. Iyengar, J. Tomasi, V. Barone, B. Mennucci, M. Cossi, G. Scalmani, N.

- Rega, G. A. Petersson, H. Nakatsuji, M. Hada, M. Ehara, K. Toyota, R. Fukuda, J. Hasegawa, M. Ishida, T. Nakajima, Y. Honda, O. Kitao, H. Nakai, M. Klene, X. Li, J. E. Knox, H. P. Hratchian, J. B. Cross, C. Adamo, J. Jaramillo, R. Gomperts, R. E. Stratmann, O. Yazyev, A. J. Austin, R. Cammi, C. Pomelli, J. W. Ochterski, P. Y. Ayala, K. Morokuma, G. A. Voth, P. Salvador, J. J. Dannenberg, V. G. Zakrzewski, S. Dapprich, A. D. Daniels, M. C. Strain, O. Farkas, D. K. Malick, A. D. Rabuck, K. Raghavachari, J. B. Foresman, J. V. Ortiz, Q. Cui, A. G. Baboul, S. Clifford, J. Cioslowski, B. B. Stefanov, G. Liu, A. Liashenko, P. Piskorz, I. Komaromi, R. L. Martin, D. J. Fox, T. Keith, M. A. Al-Laham, C. Y. Peng, A. Nanayakkara, M. Challacombe, P. M. W. Gill, B. Johnson, W. Chen, M. W. Wong, C. Gonzalez, J. A. Pople, Gaussian, Inc., Wallingford CT, 2004.
- [15] For the 6-311G(3d) basis sets see, a) R. C. Binning Jr. , L. A. Curtiss, *J. Comput. Chem.* **1990**, *11*, 1206–1216; b) L. A. Curtiss, M. P. McGrath, J.-P. Blaudeau, N. E. Davis, R. C. Binning Jr. , L. Radom, *J. Chem. Phys.* **1995**, *103*, 6104–6113; c) M. P. McGrath, L. Radom, *J. Chem. Phys.* **1991**, *94*, 511–516. For the diffuse functions (+ and++) see, T. Clark, J. Chandrasekhar, G. W. Spitznagel, P. von R. Schleyer, *J. Comput. Chem.* **1983**, *4*, 294–301.
- [16] C. C. J. Roothaan, *Rev. Mod. Phys.* **1951**, *23*, 69–89. See also *Modern Quantum Chemistry: Introduction to Advanced Electronic Structure Theory* (Eds.: A. Szabo, N. S. Ostlund), Macmillan Publishing, New York, 1982.
- [17] C. Møller, M. S. Plesset, *Phys. Rev.* **1934**, *46*, 618–622; J. Gauss, *J. Chem. Phys.* **1993**, *99*, 3629–3643; J. Gauss, *Ber. Bunsenges. Phys. Chem.* **1995**, *99*, 1001–1008.
- [18] a) A. D. Becke, *Phys. Rev. A* **1988**, *38*, 3098–3100; A. D. Becke, *J. Chem. Phys.* **1993**, *98*, 5648–5652; b) C. Lee, W. Yang, R. G. Parr, *Phys. Rev. B* **1988**, *37*, 785–789; B. Mehlrich, A. Savin, H. Stoll, H. Preuss, *Chem. Phys. Lett.* **1989**, *157*, 200–206.
- [19] For the pure p atomic orbitals, Equation (10) will fold for an example: $\langle 4p_x | L_z r^{-3} | 4p_y \rangle = \langle 4p_x | r^{-3} | 4p_x \rangle \langle 4p_x | L_z | 4p_y \rangle$ (10)
- [20] For a similar utility program based on Gaussian 98 program (NMRANAL-NH98G), see ref. [12b].
- [21] The $\psi_i \rightarrow \psi_j$ transition should be described as $\psi_i \rightarrow \psi_j$ ($j \neq i$). However, we write it as $\psi_i \rightarrow \psi_j$, since the contribution from the $\psi_i \rightarrow \psi_i$ transition is intrinsically zero.
- [22] The plots could also be well analyzed by the linear and parabolic treatments.
- [23] The average values between $\langle r_{\text{Se}}^{-3} \rangle_{\text{HOMO,rel}}$ and $\langle r_{\text{Se}}^{-3} \rangle_{\text{LUMO,rel}}$ for Se^{2+} and Se^0 at the triplet state also fall on the correlation line in Figure 5 at the singlet state. The plot is shown in Figure S3 in the Supporting Information.
- [24] The x derivatives of Equations (4) and (5) at $x=0$ ($(dy/dx)_{x=0} = A_{\text{rel}}\alpha_{\text{rel}}$) correspond to the charge dependence of $\langle r_N^{-3} \rangle_{\text{rel}}$ at $Q(N)=0$. The $A_{\text{rel}}\alpha_{\text{rel}}$ values are almost equal for $N=\text{Se}$, S , and O if calculated at the DFT (B3LYP) level (Table 3). Consequently, the $A\alpha$ values would be almost proportional to $k_0(N^0) = \langle r_N^{-3} \rangle_{\text{HOMO}}(N^0)$. Therefore, the order is expressed in Equation (11):
$$A\alpha(\text{Se}) > A\alpha(\text{S}) > A\alpha(\text{O}) \quad (11)$$
- [25] In the case of H_2Se , $\psi_1 \rightarrow \psi_{14}$ are inner MOs and ψ_{15} , ψ_{16} , ψ_{17} , and ψ_{18} are mainly constructed by $4s(\text{Se})$, $4p_y(\text{Se})$, $4p_x(\text{Se})$, and $4p_z(\text{Se})$, respectively. Contributions from $\psi_1 \rightarrow \psi_{14}$, ψ_{15} , ψ_{16} , ψ_{17} , and ψ_{18} to $\sigma^0(\text{Se})$ are -7.8 , -16.0 , -254.4 , -347.6 , and -690.0 ppm, respectively, with occupied-to-occupied of 328.8 ppm, if calculated with the B3LYP/6-311+G(3d) method. $\sigma^0(\text{Se}) = -987.1$ ppm in total.
- [26] One may expect that the $\psi_{18}(\text{HOMO})$ to $\psi_{19}(\text{LUMO})$ transition is most important in SeH_2 . However, the contribution is not so large ($\sigma^0(\text{Se})_{yy} = -293$ ppm), since ψ_{19} is mainly constructed by $s(\text{Se})$. See also ref. [25].
- [27] It would be better to employ the correlation only for $G(\mathbf{A})$, since $Q(N)$ in $G(\mathbf{B})$ may change depending on the calculation methods. See also ref. [13].

Received: February 12, 2008

Published online: July 4, 2008